

Control of *Aedes aegypti* Mosquito Vector by Attempting QSAR Modeling on Phenoxyacetamide-Based Inhibitors to Target AChE1

Aaliya Naaz¹, Mohit Kumar¹, Ankita Sharma¹, Deepak Teotia¹, Sisir Nandi^{1*} and Mridula Saxena²

¹Department of Pharmaceutical Chemistry, Global Institute of Pharmaceutical Education and Research, Affiliated to Uttarakhand Technical University, Kashipur, Uttarakhand, India; ²Department of Chemistry, Amity University, Lucknow, India

ABSTRACT

Female *Aedes aegypti* and *Anopheles gambiae* mosquitoes are living vectors liable for transmitting many parasitic and dreadful viral diseases. The major target is acetyl cholinesterase (AChE) 1 enzyme for the parasite transmission. *Anopheles gambiae* carries AgAChE1 enzyme responsible for the malaria parasite whereas *Aedes aegypti* carries AaAChE1 enzyme that injects dengue, yellow fever, Zika, and chikungunya viruses to the healthy individuals. These vector-borne infections are now a major public threat. Deforestation and global warming may cause drastic change of the climate which causes vector-borne disease to re-emerge worldwide. Control of mosquito vector saves many lives. One of the mechanisms to kill the mosquito vector is to use insecticides such as chlorinated hydrocarbons, organophosphates, carbamates, and pyrethroids recommended by the World Health Organization (WHO). These are covalent inhibitors of acetyl cholinesterase enzyme and their accumulation may produce ecotoxicity to the non-targets including aquatic animals and humans. It was shown that non covalent phenoxyacetamide-based inhibitors can specifically target acetyl cholinesterase (AChE) 1 responsible for the vector transmission. Therefore, an attempt has been made to explore AChE1 target via ligand based quantitative structure-activity relationship (QSAR) modeling on phenoxyacetamide-based compounds to predict crucial features of these inhibitors responsible for the design of highly active ligands.

Keywords: *Aedes aegypti* mosquito vector; Computed structural descriptors; GA-MLR based QSAR; AChE1; Phenoxyacetamide

INTRODUCTION

Vector-borne diseases are the infections which are transmitted via living organisms that represent the vector. These vectors are mosquitoes, ticks, flies, sandflies, fleas, triatomine bugs, and some fresh water aquatic snails. The disease-vector bites an infected animal or human and then transmits pathogens through blood meals between vertebrate host animals and humans. Thus the infection spread from an infected fellow to the healthy individuals [1,2]. Vector-borne infections become a pandemic threat because more than one billion people get infected each year, engulfing more than 7,00,000 annual deaths caused by malaria, dengue, schistosomiasis, human African trypanosomiasis, leishmaniasis, Chagas disease, yellow fever, Japanese encephalitis, and onchocerciasis, globally [3]. Since 2014, outbreaks of dengue, malaria, chikungunya, yellow fever and Zika have claimed a strong helmet over the health system protection in many countries. Therefore, control of the mosquito vector is a major target nowadays [3]. Four types of insecticides including chlorinated hydrocarbons, organophosphates,

carbamate, and pyrethroids were recommended by the World Health Organization (WHO) for controlling mosquito-vectors [4,5]. These compounds can damage the neurotransmission signaling system. Acetylcholine (Ach) releases into the synaptic cleft where it binds to Ach receptors at the post-synaptic membrane, transferring the signal to downstream nerve cells. Acetyl cholinesterase (AChE) causes breakdown of the Ach to produce choline which is being re-used for further synthesis of Ach to proceed synaptic signaling system. Inhibition of AChE causes an accumulation of acetylcholine, leading to overstimulation and then paralysis of the nervous system [6,7]. Therefore, inhibition of AChE is a major target to control the mosquito vector.

Insecticide resistance and toxicity become a major drawback [8,9]. To quest least toxic chemicals, covalent inhibitors such as carbamate derivatives and difluoromethyl ketones were being developed as inhibitors of AChE1 and AChE2 enzymes responsible for transmission of vector found in *Anopheles gambiae* (AgAChE1; vector of the malaria parasite) and *Aedes aegypti* (AaAChE1; vector of

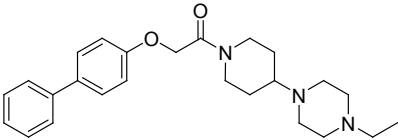
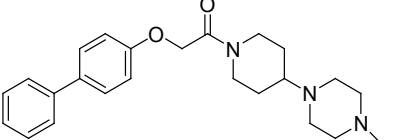
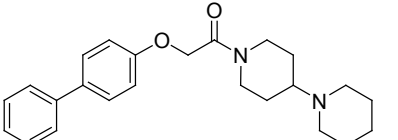
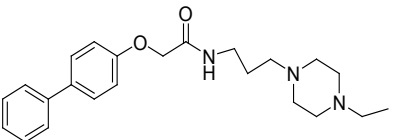
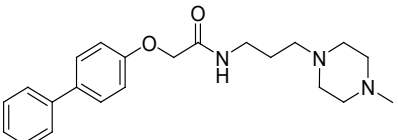
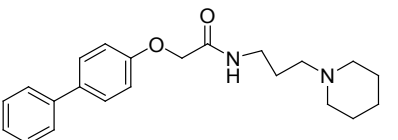
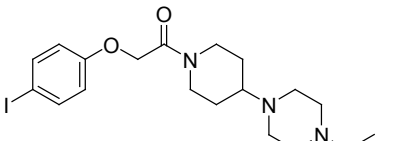
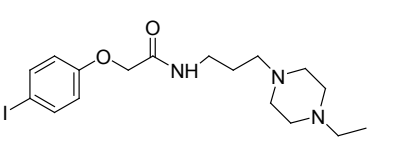
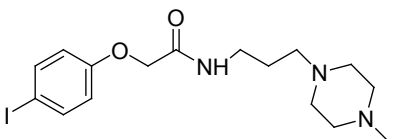
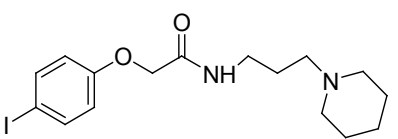
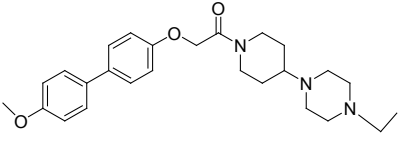
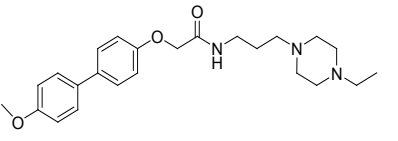
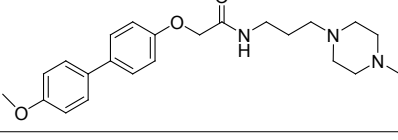
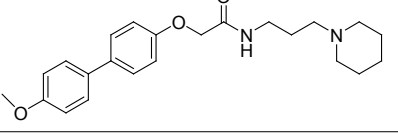
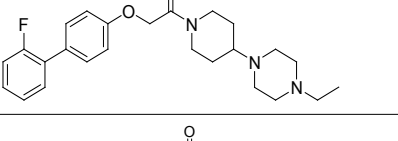
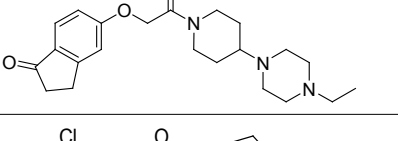
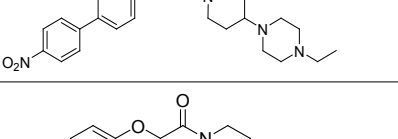
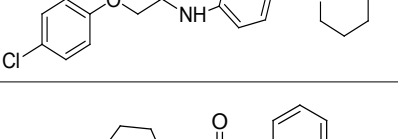
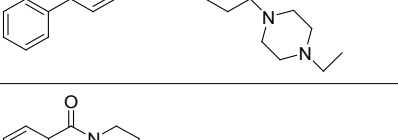
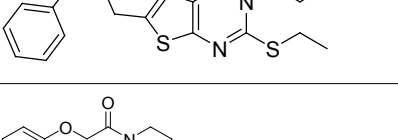
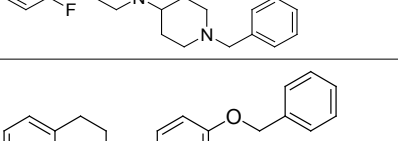
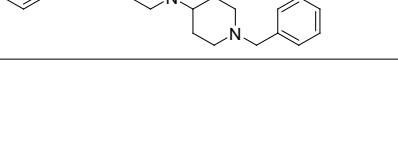
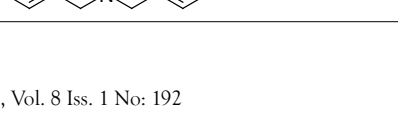
Correspondence to: Sisir Nandi, Department of Pharmaceutical Chemistry, Global Institute of Pharmaceutical Education and Research, Affiliated to Uttarakhand Technical University, Kashipur-244713, Uttarakhand, India, Tel: +91 7500458478; E-mail: sisir.iicb@gmail.com

Received: February 26, 2019; **Accepted:** March 05, 2019; **Published:** March 12, 2019

Citation: Naaz A, Kumar M, Sharma A, Teotia D, Nandi S, Saxena M (2019) Control of *Aedes aegypti* Mosquito Vector by Attempting QSAR Modeling on Phenoxyacetamide-Based Inhibitors to Target AChE1. J Develop Drugs 8:192. doi: 10.4172/2329-6631.1000192

Copyright: © 2019 Naaz A, et al. This is an open-access article distributed under the terms of the Creative Commons Attribution License, which permits unrestricted use, distribution, and reproduction in any medium, provided the original author and source are credited.

Table 1: Biological activity data.

Comp No.	Structure	pIC ₅₀ (μM)	Comp No.	Structure	pIC ₅₀ (μM)
1.		0.657	2.		0.602
3.		-0.602	4.		-0.518
5.		-1.079	6.		-0.995
7.		-0.176	8.		-1.857
9.		-2.049	10.		-1.556
11.		0.638	12.		-0.579
13.		-1.204	14.		-0.591
15.		0.657	16.		0.698
17.		0.958	18.		0.356
19.		0.657	20.		-0.944
21.		-1.079	22.		-1.278
23.		-0.462			

the dengue, yellow fever, Zika, and chikungunya viruses). But these compounds failed due to lack of desired selectivity and potency [10-12]. Therefore, much more attention was paid nowadays on to the discovery of non-covalent inhibitors acetylcholinesterase 1 (AChE1) as the role of AChE2 is still not fully understood [13-18].

Alout et al. [19] tested a non-covalent, reversible class of pyrimidinetrion furan-substituted compounds that showed promising potency on AgAChE1 and AgAChE1-G122S both *in vitro* and on mosquito larvae, however, the selectivity profile of these compounds was not reported. Knutsson and co-workers [20] developed many N-aryl-N'-ethyleneaminothioureas which proved to be inhibitors of AChE1; the most efficient following compound showed sub-micromolar potency. Importantly, the inhibitors exhibited selectivity over the human AChE (hAChE), which is desirable for new insecticides. The structure-activity relationship (SAR) analysis of the thioureas revealed that small changes in

the chemical structure had a large effect on inhibition capacity. Knutsson et al. [21] recently discovered a number of non-covalent inhibitors that selectively target Acetylcholinesterase 1 (AChE1) of the mosquitoes *An. gambiae* and *Aedes aegypti* (*Ae. aegypti*, transmitting dengue, chikungunya, and Zika virus infections). AChE1 is a validated insecticide target to control mosquito vectors of e.g., malaria, dengue, and Zika virus infections. The insecticides most commonly used for vector control disrupt the insect's nervous system by inhibiting voltage-gated ion channels (pyrethroids and organochlorines) or by inhibiting the essential enzyme acetylcholinesterase (AChE) (organophosphates and carbamates). The physiological role of AChE is to terminate nerve signaling by rapidly hydrolyzing the neurotransmitter acetylcholine. The design, synthesis, *in vitro* and *in vivo* evaluation of phenoxyacetamide-based analogs were done. The aim was to explore the molecular basis for the inhibitors' selectivity for mosquito AChE1 versus hAChE and their potency on G122S mutated AgAChE1. In a recent

Table 2: Best QSAR models.

Model-1	
$pIC_{50} = 8.168(+/-1.164) - 0.001(+/-0.0001) ATSC8m - 1.147(+/-0.957) VE1_Dze - 19.051(+/-2.633) E2e$ N=16, R ² =0.867, Q ² _{Loo} =0.809, R ² _{pred} =0.591, r ² _m (test)=0.686, SEE=0.323	
Parameters	Physical interpretation
ATSC8m	Centered Broto-Moreau autocorrelation of lag 8 weighted by mass
VE1_Dze	The coefficient sum of the last eigenvector from Barysz matrix / weighted by Sanderson electronegativities
E2e	2nd component accessibility directional WHIM index / weighted by Sanderson electronegativity
Model-2	
$pIC_{50} = -3.456(+/-2.773) - 0.966(+/-0.299) TDB9r - 8.403(+/-0.795) E2v + 2.475(+/-0.787) SpMax6_Bhi$ N=14, R ² =0.938, Q ² _{Loo} =0.882, R ² _{pred} =0.789, r ² _m (test)=0.578, SEE=0.211	
Parameters	Physical interpretation
TDB9r	3D Topological distance based descriptors - lag 9 weighted by covalent radius
E2v	2nd component accessibility directional WHIM index / weighted by van der Waals volume
SpMax6_Bhi	largest eigenvalue n. 6 of Burden matrix weighted by ionization potential
Model-3	
$pIC_{50} = 1.127(+/-0.518) + 0.101(+/-0.019) RDF90u + 1.447(+/-0.818) E2m - 10.835(+/-1.504) E2v$ N=17, R ² =0.890, Q ² _{Loo} =0.803, R ² _{pred} =0.946, r ² _m (test)=0.871, SEE=0.313	
Parameters	Physical interpretation
RDF90u	Radial distribution function - 090 / unweighted
E2m	2 nd component accessibility directional WHIM index / weighted by mass
E2v	2 nd component accessibility directional WHIM index / weighted by van der Waals volume

Table 3: Pearson correlation coefficient between the modeled descriptors.

Parameters of model 1			
Parameters	ATSC8m	VE1_DZe	E2
ATSC8m	1.00	-	-
VE1_DZe	-0.411	1.00	-
E2	-0.117	0.330	1.00
Parameters of model 2			
Parameters	TDB9r	E2v	SpMax6_Bhi
TDB9r	1.00	-	-
E2v	-0.159	1.00	-
SpMax6_Bhi	-0.167	-0.545	1.00
Model Parameters of model 2			
Parameters	RDF90u	E2m	E2v
RDF90u	1.00	-	-
E2m	-0.157	1.00	-
E2v	-0.123	0.602	1.00

ALogP, ALogp2, AMR, apol, naArom, Atom, nAtom, nHeavyAtom, nH, nC, nN, nO, nS, nF, nCl, nI, nX, AT50m, AT51m, AT52m, AT53m, AT54m, AT55m, AT56m, AT57m, AT58m, AT59m, AT50v, AT51v, AT52v, AT53v, AT54v, AT55v, AT56v, AT57v, AT58v, AT59v, AT50s, AT51s, AT52s, AT53s, AT54s, AT55s, AT56s, AT57s, AT58s, AAT50m, AAT51m, AAT52m, AAT53m, AAT54m, AAT55m, AAT56m, AAT57m, AAT58m, AAT59v, AAT51v, AAT52v, AAT53v, AAT54v, AAT55v, AAT56v, AAT57v, AAT58v, AAT59e, AAT50e, AAT51e, AAT52e, AAT53e, AAT54e, AAT55e, AAT56e, AAT57e, AAT58e, AAT59e, AAT50i, AAT51i, AAT52i, AAT53i, AAT54i, AAT55i, AAT56i, AAT57i, AAT58i, AAT59s, AAT50s, AAT51s, AAT52s, AAT53s, AAT54s, AAT55s, AAT56s, AAT57s, AAT58s, ATSC0, ATSC1c, ATSC2c, ATSC3c, ATSC4c, ATSC5c, ATSC6c, ATSC7c, ATSC8c, ATSC1m, ATSC2m, ATSC3m, ATSC4m, ATSC5m, ATSC6m, ATSC7m, ATSC8m, ATSC0v, ATSC1v, ATSC2v, ATSC3v, ATSC4v, ATSC5v, ATSC6v, ATSC7v, ATSC8v, ATSC0e, ATSC1e, ATSC2e, ATSC3e, ATSC4e, ATSC5e, ATSC6e, ATSC7e, ATSC8e, ATSC0p, ATSC1p, ATSC2p, ATSC3p, ATSC4p, ATSC5p, ATSC6p, ATSC7p, ATSC8p, ATSC0i, ATSC1i, ATSC2i, ATSC3i, ATSC4i, ATSC5i, ATSC6i, ATSC7i, ATSC8i, ATSC0s, ATSC1s, ATSC2s, ATSC3s, ATSC4s, ATSC5s, ATSC6s, ATSC7s, ATSC8s, AATSC1m, AATSC3m, AATSC4m, AATSC5m, AATSC6m, AATSC7m, AATSC8m, AATSC0v, AATSC1v, AATSC2v, AATSC3v, AATSC4v, AATSC5v, AATSC6v, AATSC7v, AATSC8v, AATSC0e, AATSC1e, AATSC2e, AATSC3e, AATSC4e, AATSC5e, AATSC6e, AATSC7e, AATSC8e, AATSC0p, AATSC1p, AATSC2p, AATSC3p, AATSC4p, AATSC5p, AATSC6p, AATSC7p, AATSC8p, AATSC0i, AATSC1i, AATSC2i, AATSC3i, AATSC4i, AATSC5i, AATSC6i, AATSC7i, AATSC8i, AATSC0s, AATSC1s, AATSC2s, AATSC3s, AATSC4s, AATSC5s, AATSC6s, AATSC7s, AATSC8s, MATS1c, MATS2c, MATS3c, MATS4c, MATS5c, MATS6c, MATS8c, MATS1m, MATS2m, MATS3m, MATS4m, MATS5m, MATS6m, MATS7m, MATS8m, MATS5v, MATS1e, MATS2e, MATS3e, MATS4e, MATS5e, MATS6e, MATS7e, MATS8e, MATS1p, MATS2p, MATS3p, MATS4p, MATS5p, MATS6p, MATS7p, MATS8p, MATS1i, MATS4i, MATS7i, MATS8i, MATS1s, MATS2s, MATS3s, MATS4s, MATS5s, MATS6s, MATS7s, MATS8s, GATS1c, GATS2c, GATS3c, GATS4c, GATS5c, GATS6c, GATS7c, GATS8c, GATS1m, GATS2m, GATS3m, GATS4m, GATS5m, GATS6m, GATS7m, GATS8m, GATS1v, GATS2v, GATS3v, GATS4v, GATS5v, GATS6v, GATS7v, GATS8v, GATS1e, GATS2e, GATS3e, GATS4e, GATS5e, GATS6e, GATS7e, GATS8e, GATS1p, GATS2p, GATS3p, GATS4p, GATS5p, GATS6p, GATS7p, GATS8p, GATS1i, GATS2i, GATS3i, GATS4i, GATS5i, GATS6i, GATS7i, GATS8i, GATS1s, GATS2s, GATS3s, GATS4s, GATS5s, GATS6s, GATS7s, GATS8s, SpAbs_DzZ, SpMAD_DzZ, SM1_DzZ, VE1_DzZ, VE3_DzZ, VR1_DzZ, VR3_DzZ, SpDiam_Dzv, SpMAD_Dzv, SM1_Dzv, VE1_Dzv, VE3_Dzv, VR1_Dzv, VR2_Dzv, VR3_Dzv, SM1_Dze, VE1_Dze, VE3_Dze, SpMAD_Dzp, SM1_Dzp, VE1_Dzp, VE3_Dzp, VR1_Dzp, VR2_Dzp, VR3_Dzp, SpMAD_Dzi, SM1_Dzi, VE1_Dzi, VE3_Dzi, VR1_Dzi, VR2_Dzi, VR3_Dzi, SpAbs_Dzs, SpDiam_Dzs, SpMAD_Dzs, SM1_Dzs, VE1_Dzs, VE3_Dzs, VR1_Dzs, VR2_Dzs, VR3_Dzs, nBase, BCUTw-1l, BCUTc-1l, BCUTc-1h, BCUTp-1l, BCUTp-1h, nBonds, nBonds2, nBonds3, nBondsD, nBondsD2, nBondsM, bpol, SpMax2_Bhm, SpMax3_Bhm, SpMax4_Bhm, SpMax5_Bhm, SpMax6_Bhm, SpMax7_Bhm, SpMax8_Bhm, SpMin1_Bhm, SpMin2_Bhm, SpMin3_Bhm, SpMin4_Bhm, SpMin5_Bhm, SpMin6_Bhm, SpMin7_Bhm, SpMin8_Bhm, SpMax1_Bhv, SpMax2_Bhv, SpMax3_Bhv, SpMax4_Bhv, SpMax5_Bhv, SpMax6_Bhv, SpMax7_Bhv, SpMax8_Bhv, SpMin1_Bhv, SpMin2_Bhv, SpMin3_Bhv, SpMin4_Bhv, SpMin5_Bhv, SpMin6_Bhv, SpMin7_Bhv, SpMin8_Bhv, SpMax1_Bhe, SpMax2_Bhe, SpMax3_Bhe, SpMax4_Bhe, SpMax5_Bhe, SpMax6_Bhe, SpMax7_Bhe, SpMax8_Bhe, SpMin1_Bhe, SpMin2_Bhe, SpMin3_Bhe, SpMin4_Bhe, SpMin5_Bhe, SpMin6_Bhe, SpMin7_Bhe, SpMin8_Bhe, SpMax1_Bhp, SpMax2_Bhp, SpMax3_Bhp, SpMax4_Bhp, SpMax5_Bhp, SpMax6_Bhp, SpMax7_Bhp, SpMax8_Bhp, SpMin2_Bhp, SpMin3_Bhp, SpMin4_Bhp, SpMin5_Bhp, SpMin6_Bhp, SpMin7_Bhp, SpMin8_Bhp, SpMax1_Bhi, SpMax2_Bhi, SpMax3_Bhi, SpMax4_Bhi, SpMax5_Bhi, SpMax6_Bhi, SpMax7_Bhi, SpMax8_Bhi, SpMin2_Bhi, SpMin3_Bhi, SpMin4_Bhi, SpMin6_Bhi, SpMin7_Bhi, SpMin8_Bhi, SpMax1_Bhs, SpMax2_Bhs, SpMax3_Bhs, SpMax4_Bhs, SpMax5_Bhs, SpMax6_Bhs, SpMax7_Bhs, SpMax8_Bhs, SpMin1_Bhs, SpMin2_Bhs, SpMin3_Bhs, SpMin4_Bhs, SpMin5_Bhs, SpMin6_Bhs, SpMin7_Bhs, SpMin8_Bhs, C1SP2, C2SP2, C3SP2, C1SP3, C2SP3, SCH-5, SCH-6, SCH-7, VCH-5, VCH-6, VCH-7, SC-3, SC-5, VC-3, VC-5, SPC-4, SPC-5, SPC-6, VPC-4, VPC-5, VPC-6, SP-0, SP-2, SP-3, SP-4, SP-5, SP-6, ASP-0, ASP-2, ASP-3, VP-0, VP-1, VP-2, VP-3, VP-4, VP-5, VP-6, VP-7, AVP-0, AVP-1, AVP-2, VP-3, Sv, Mv, Mp, CrippenLogP, CrippenMR, SpMax_Dt, SpDiam_Dt, SpMAD_Dt, VE1_Dt, VE3_Dt, VR1_Dt, VR2_Dt, VR3_Dt, ECCEN, nHBd, nHBa, nWBa, nHBint4, nHBint7, nHdCH, nHaaCH, nHCsats, nHCsatu, nHother, nsCH3, nsSCH2, nsSSCH, ndssC, naasC, nsSSNdO, nssO, nsOm, SHBa, SwHBA, SHaaCH, SHCsats, SHCsatu, SHother, SsCH3, SssCH2, SdssC, SaasC, SdO, minHBA, minwHBA, minHdsCH, minHaaCH, minHCsats, minHCsatu, minHother, minSCH3, minssCH2, mindssCH, minaaCH, mindssC, minaaC, mindO, minssO, maxHBA, maxwHBA, maxHaaCH, maxHCsats, maxHCsatu, maxHother, maxsCH3, maxssCH2, maxaaCH, maxdssC, maxaaC, maxsssN, maxsSO, suml, meanl, hmax, hmin, gmin, LipoaffinityIndex, MAXDN, MAXDP, DELS, MAXDN2, DELS2, ETA_Alpha, ETA_AlphaP, ETA_dAlpha_B, ETA_Epsilon_1, ETA_Epsilon_2, ETA_Epsilon_3, ETA_Epsilon_4, ETA_Epsilon_5, ETA_dEpsilon_A, ETA_dEpsilon_B, ETA_dEpsilon_C, ETA_Psi_1, ETA_Shape_P, ETA_Shape_Y, ETA_Beta, ETA_BetaP, ETA_Beta_s, ETA_BetaP_s, ETA_Beta_ns, ETA_BetaP_ns, ETA_dBeta, ETA_dBetaP, ETA_Beta_ns_d, ETA_BetaP_ns_d, ETA_Eta, ETA_EtaP, ETA_Eta_R, ETA_Eta_F, ETA_Eta_P, ETA_Eta_L, ETA_Eta_P_L, ETA_Eta_F_L, ETA_Eta_P_L, ETA_Eta_B, ETA_Eta_B_RC, FMF, fragC, nHBacc, nHBacc2, nHBacc3, nHBacc_Lipinski, HybRatio, IC0, IC1, IC2, IC3, IC4, IC5, TIC0, TIC1, TIC2, TIC3, TIC4, TIC5, SIC0, SIC1, SIC2, SIC3, SIC4, SIC5, CIC0, CIC1, CIC2, CIC3, CIC4, CIC5, BIC1, BIC2, BIC3, BIC4, BIC5, MIC0, MIC1, MIC2, MIC3, ZMIC1, ZMIC2, ZMIC3, ZMIC4, ZMIC5, Kier1, Kier2, Kier3, nAtomLC, nAtomP, nAtomLAC, MLogP, McGowan_Volume, MDEC-11, MDEC-13, MDEC-22, MDEC-23, MDEC-33, MDEO-11, MDEO-12, MDEO-22, MDEN-23, MDEN-33, MLFER_A, MLFER_BH, MLFER_S, MLFER_L, MPC3, MPC4, MPC6, MPC8, TPC, piPC1, piPC2, piPC4, piPC5, piPC6, piPC9, R_TpiPCTPC, PetitjeanNumber, nRing, n5Ring, n6Ring, nFRing, nF9Ring, nF10Ring, nTRing, nHeteroRing, n6HeteroRing, nRotB, RotBfrac, nRotBt, RotBtfrac, LipinskiFailures, topoRadius, topoDiameter, GGI1, GGI2, GGI3, GGI4, GGI5, GGI6, GGI7, GGI8, GGI9, GGI10, JGI1, JGI2, JGI3, JGI4, JGI5, SpMAD_D, VE1_D, VE3_D, VR1_D, VR2_D, VR3_D, TopoPSA, MWC2, MWC4, MWC6, MWC10, MW, AMW, WTPT-2, WTPT-3, WTPT-5, WPATH, WPOL, XLogP, TDB1u, TDB2u, TDB3u, TDB4u, TDB5u, TDB6u, TDB7u, TDB8u, TDB9u, TDB10u, TDB5m, TDB6m, TDB7m, TDB8m, TDB9m, TDB10m, TDB1v, TDB2v, TDB3v, DB4v, TDB5v, TDB6v, TDB7v, TDB8v, TDB9v, TDB10v, TDB1e, TDB2e, TDB3e, TDB4e, TDB5e, TDB6e, TDB7e, TDB8e, TDB9e, TDB10e, TDB1p, TDB2p, TDB3p, TDB4p, TDB5p, TDB6p, TDB7p, TDB8p, TDB9p, TDB10p, TDB1i, TDB2i, TDB3i, TDB4i, TDB5i, TDB6i, TDB7i, TDB8i, TDB9i, TDB10i, TDB1s, TDB2s, TDB3s, TDB4s, TDB5s, TDB6s, TDB7s, TDB8s, TDB9s, TDB10s, TDB1r, TDB2r, TDB3r, TDB4r, TDB5r, TDB6r, TDB7r, TDB8r, TDB9r, TDB10r, PPSA-1, PPSA-2, PPSA-3, PNSA-1, PNSA-2, PNSA-3, DPSSA-1, DPSSA-2, DPSSA-3, FPSA-1, FPSA-2, FPSA-3, WPSA-1, WPSA-2, WPSA-3, WNSA-1, WNSA-2, WNSA-3, RPCG, RNCG, RPCS, RNCS, THSA, TPSA, RNSA, GRAV-1, GRAVH-1, GRAV-4, LOBMAX, MOMI-X, MOMI-Y, MOMI-Z, MOMI-XY, MOMI-XZ, MOMI-R, geomRadius, geomDiameter, geomShape, RDF10u, RDF15u, RDF20u, RDF25u, RDF30u, RDF35u, RDF40u, RDF45u, RDF50u, RDF55u, RDF60u, RDF65u, RDF70u, RDF75u, RDF80u, RDF85u, RDF90u, RDF95u, RDF100u, RDF105u, RDF110u, RDF115u, RDF120u, RDF125u, RDF130u, RDF135u, RDF140u, RDF145u, RDF150u, RDF155u, RDF160m, RDF20m, RDF25m, RDF30m, RDF35m, RDF40m, RDF45m, RDF50m, RDF55m, RDF60m, RDF65m, RDF70m, RDF75m, RDF80m, RDF85m, RDF90m, RDF95m, RDF100m, RDF105m, RDF110m, RDF115m, RDF120m, RDF125m, RDF130m, RDF135m, RDF140m, RDF145m, RDF150m, RDF155m, RDF160v, RDF15v, RDF20v, RDF25v, RDF30v, RDF35v, RDF40v, RDF45v, RDF50v, RDF55v, RDF60v, RDF65v, RDF70v, RDF75v, RDF80v, RDF85v, RDF90v, RDF95v, RDF100v, RDF105v, RDF110v, RDF115v, RDF120v, RDF125v, RDF130v, RDF135v, RDF140v, RDF145v, RDF150v, RDF155v, RDF160e, RDF80e, RDF90e, RDF95e, RDF100e, RDF20p, RDF30p, RDF35p, RDF40p, RDF45p, RDF50p, RDF55p, RDF60p, RDF65p, RDF70p, RDF75p, RDF80p, RDF85p, RDF90p, RDF95p, RDF100p, RDF105p, RDF110p, RDF115p, RDF120p, RDF130p, RDF135p, RDF140p, RDF145p, RDF150p, RDF155p, RDF160i, RDF15i, RDF20i, RDF25i, RDF40i, RDF45i, RDF95i, RDF105i, RDF115i, RDF125i, RDF135i, RDF145i, RDF155i, RDF160s, RDF15s, RDF20s, RDF25s, RDF30s, RDF35s, RDF40s, RDF45s, RDF50s, RDF55s, RDF60s, RDF65s, RDF70s, RDF75s, RDF80s, RDF85s, RDF90s, RDF95s, RDF100s, RDF105s, RDF110s, RDF115s, RDF120s, RDF125s, RDF130s, RDF135s, RDF140s, RDF145s, RDF150s, RDF155s, L1u, L2u, L3u, P1u, P2u, E1u, E2u, E3u, Au, Vu, Du, L1m, L2m, L3m, P1m, P2m, E1m, E2m, E3m, Tm, Am, Vm, Dm, L1v, L2v, L3v, P1v, P2v, F1v, F2v, F3v, Av, Vv, Dv, L2e, F1e, F2e, F3e, De, L2p, F1p, F2p, F3p, Tp, Ap, Vp, Dp, F1i, F2i, Di, F1s, F2s, Ds.

Figure 1: Descriptors used in current study.

differential high-throughput screen (HTS) studied against the AChE1 enzymes from *Anopheles gambiae* (*An. gambiae*; vector of the malaria parasite; AgAChE1) and *Aedes aegypti* (*Ae. aegypti*; vector of the dengue, yellow fever, chikungunya, and Zika virus infection; AaAChE1), Engdahl et al. identified a number of non-covalent phenoxyacetamide based hits showing potential selectivity for the mosquito enzymes over the human enzyme [22]. But there is hardly any QSAR formulated on these compounds till date. Therefore, it is our target in the present study to explore structural features for the design of congeneric potent phenoxyacetamide compounds to inhibit AChE1 responsible for the transmission of ZIKV mosquito vector.

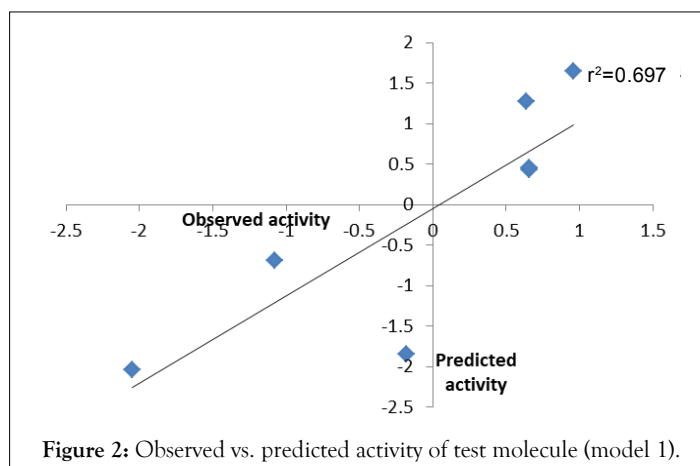


Figure 2: Observed vs. predicted activity of test molecule (model 1).

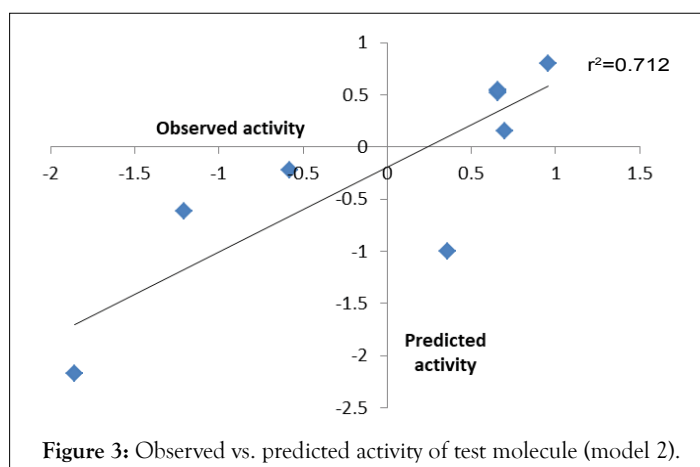


Figure 3: Observed vs. predicted activity of test molecule (model 2).

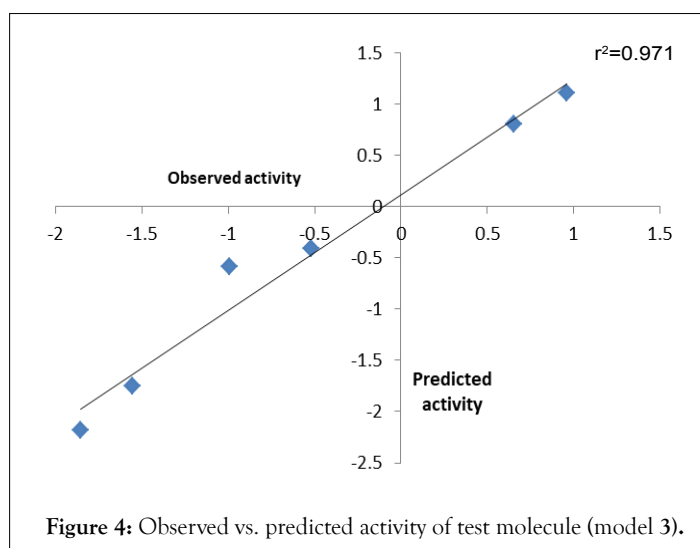


Figure 4: Observed vs. predicted activity of test molecule (model 3).

MATERIALS AND METHODS

Biological activity data

A total number of 23 phenoxyacetamide derivatives (Table 1) showing half maximum inhibitory effect on enzyme acetylcholinesterase 1 (AChE1) of AaAChE1 that represents *Aedes aegypti* (*Ae. aegypti*; vector of the dengue, yellow fever, chikungunya, and Zika virus infection). The design, synthesis and *in vitro* activity evaluation of phenoxyacetamide-based analogs were done to explore the molecular basis for the inhibitors' selectivity towards mosquito AChE1 [21,22]. These inhibitors target the essential enzyme acetylcholinesterase which terminates cholinergic transmission through rapid hydrolysis of the neurotransmitter acetylcholine.

Structure formulation and calculation of molecular descriptors

All the structures of 23 phenoxyacetamide derivatives were formulated using 2D ChemDraw. The 2D structures were then converted into 3D modules and the geometries of all compounds were fully minimized using MM2 force field considering the default conversion procedure [23]. Fully optimized 3D structures were browsed into PaDEL descriptor which is freely accessible open source software for calculation of theoretical molecular descriptors classification into 1D, 2D, and 3D respectively. Many 1875 structural invariants were calculated using the Chemistry Development Kit based on the code of Java language [24,25].

Theoretical molecular descriptors or the structural invariants encode molecular configuration and properties in terms of physicochemical constitutional, geometrical and three dimensional (3D), electrostatic, functional, atom centered fragments and topological indices, respectively. Biological activity (pIC_{50}) is quantitatively correlated with various structural invariants to formulate QSAR model in terms of statistical regression methods. QSAR based on computed structure descriptors may provide a significant tool for the rational design of potent molecule in theoretical drug design and discovery research [26-31].

Statistical GA-MLR modeling

1875 descriptors were calculated and reduced to 1071. The reduced set of theoretical molecular descriptors (Figure 1) was taken into consideration for the development of a quantitative structure-activity relationship model. Descriptors with perfectly constant and highly inter-correlated descriptors were removed considering variance and correlation coefficient cut-off values of 0.0001 and 0.99 using V-WSP algorithm of Nanobridges software [32]. The reason is that the highly inter-correlated descriptors may contribute chance correlation and produce overfitting of the model. As the number of structural predictors greatly exceeds the number of compounds, the selection of important predictors is necessary for the QSAR modeling. Genetic algorithm-multiple linear regression (GA-MLR) has been used for the development of QSAR model considering reduced predictors data after variable selection by genetic algorithm method [33,34]. The GA methods uses a binary string of digits containing the values of "1" or "0" for presence and absence of the invariant. The length of each string is the same and is equal to the total number of descriptors. Quality of the model is calculated by the fitness function by taking 100 different random combinations of the calculated molecular descriptors.

Fitness function of each model is formulated in term of Q^2_{Loo} or R^2 where, Q^2_{Loo} represents cross-validated R^2 . Values of Q^2_{Loo} and R^2 are calculated by the standard equation [27,35,36].

RESULTS AND DISCUSSION

Total data set comprise of 23 phenoxyacetamide compounds. A number of training and test set was randomly generated. Many training QSAR models have been developed utilizing various sets of computed molecular descriptors including 1D, 2D, and 3D respectively using GA-MLR methods of NanoBridges software. The impact of the different classes of computed descriptors on the inhibition of acetylcholinesterase1 (AChE1) by phenoxyacetamide compounds has been carried out. It was shown that combination of 1D, 2D and 3D descriptors give highest AChE1 inhibitory impact in terms of good quality model evaluation parameters denoted by R^2 (R is the square root of multiple R-square for regression), Q^2_{Loo} (cross-validated r^2) values for the training set, an external validation was performed by calculating predictive R^2 (R^2_{pred}) and the standard error of estimation, SEE, and modified r^2 (r^2_{m}). R^2 , Q^2_{Loo} , R^2_{pred} , and r^2_{m} are calculated by using standard statistical equations [27,35-38]. The value of R^2 should be greater than 0.6, whereas Q^2_{Loo} , R^2_{pred} [37,38] and r^2_{m} which denotes predictive statistics should be greater than 0.5 [39]. Since the data set is small (only 23 compounds), three QSAR models with 3 different test set compounds showing the best results on the AChE1 synthesis inhibition is given in Table 2.

The training model 1 is based on 70% of total data set whereas model 2 is formulated using 61% of the total data set. The compound numbers 1, 5, 7, 9, 11, 15 and 17 were treated as a test set for model 1 whereas molecule number 1, 8, 12-13 and 15-19 were taken as a test set in case of development of QSAR model 2. Model 3 consists of 74% and 26% as training and test set of the total data. Test set molecules are 1, 4, 6, 8, 10 and 17. So diversity is there for the training and test set generation. R^2 , Q^2_{Loo} , R^2_{pred} , and r^2_{m} for all models 1-3 are acceptable.

Further, the Pearson correlation coefficient between the descriptors which arrived in the best QSAR models 1-3 are given in Table 3. It was shown that chance correlation is zero for the developed models 1-3 because the correlation between the descriptors was calculated as ≤ 0.33 except E2v and E2m which shows 0.602. It is also acceptable.

To examine the further predictive power of the models, QSARs 1-3 are used to predict the biological activities of the corresponding test sets. Correlation between observed and predicted activities was graphically plotted in (Figures 2-4). The square correlation coefficient (r^2) between observed vs. predicted activities were calculated as 0.697, 0.712 and 0.971 respectively which stands significant model validation.

From the QSAR results, it was shown that ATSC8m, VE1_Dze, E2e, TDB9r, SpMax6_Bhi, RDF90u, E2m, and E2v are important descriptors captured in the training QSAR models 1-3 responsible for producing inhibition of target enzyme AChE1.

CONCLUSION

QSARs 1-3 depicted that these molecules should produce the ionizing potential which represents electronegativities and electrostatics interaction towards receptors. It was captured by modeled parameters including VE1_Dze, E2e, E2v, SpMax6_Bhi and RDF90u invariants of the phenoxyacetamide. From the above

QSAR study, it was predicted that these compounds should not produce covalent linkage towards AChE1. It is denoted by the property TDB9r with negative regression coefficient which focuses on 3D topological radius distance based covalent radius already captured in QSAR model 2.

Out of these three QSAR, model 3 represents the best results. The modeled parameters RDF90u encodes radial distribution function which is correlated with the electronegativities due to electron delocalization. The parameter E2m representing 2nd component accessibility directional WHIM index/weighted by mass encodes the atomic distribution and shape. In this QSAR study, it was also found that the groups having higher van der Waals radius are not favorable. Therefore small electron-withdrawing groups such as Cl, Br, F, and CCl_3 responsible for electron delocalization may be favorable to produce potent congeneric phenoxyacetamide compounds having inhibition of AChE1 enzyme. Thus it is an attempt to Control of *Aedes aegypti* mosquito vector transmitting dengue, yellow fever, chikungunya, and Zika virus infection.

REFERENCES

1. WHO. A global brief on vector-borne diseases. World Health Organization. 2014;2:1.
2. Verwoerd DW. Definition of a vector and a vector-borne disease. Revue scientifique et technique (International Office of Epizootics). 2015;34:29-39.
3. WHO. Vector-borne diseases. 2017;2:1.
4. Najera JA, Zaim M. Malaria vector control: Insecticides for indoor residual spraying. World Health Organization Pesticide Evaluation Scheme. 2001.
5. Casida JE, Quistad GB. Golden age of insecticide research: Past, present, or future?. Annu Rev Entomol. 1998;43:1-16.
6. Berg HV, Zaim M, Yadav RS, Soares A, Ameneshewa B, et al. Global trends in the use of insecticides to control vector-borne diseases. Environ Health Perspect. 2012;120:577-582.
7. Casida JE, Durkin KA. Neuroactive insecticides: Targets, selectivity, resistance, and secondary effects. Annu Rev Entomol. 2013;58:99-117.
8. Hemingway J, Hawkes NJ, McCarroll L, Ranson H. The molecular basis of insecticide resistance in mosquitoes. Insect Biochem Mol Biol. 2004;34:653-665.
9. Rivero A, Vezilier J, Weill M, Read AF, Gandon S. Insecticide control of vector-borne diseases: When is insecticide resistance a problem?. PLoS Pathog. 2010;6:e1001000.
10. Fukuto TR. Mechanism of action of organophosphorus and carbamate insecticides. Environ Health Perspect. 1990;87:245-254.
11. Colovic MB, Krstic DZ, Lazarevic-Pasti TD, Bondzic AM, Vasic VM. Acetylcholinesterase inhibitors: Pharmacology and toxicology. Curr Neuropharmacol. 2013;11:315-335.
12. Jiang Y, Swale D, Carlier PR, Hartsel JA, Ma M, et al. Evaluation of novel carbamate insecticides for neurotoxicity to non-target species. Pestic Biochem Physiol. 2013;106:156-161.
13. Anthony N, Rocheleau T, Mocelin G, Lee HJ, French-Constant R. Cloning, sequencing and functional expression of an acetylcholinesterase gene from the yellow fever mosquito *Aedes aegypti*. FEBS Lett. 1995;368:461-465.
14. Mori A, Lobo NF, De-Bruyn B, Severson DW. Molecular cloning and characterization of the complete acetylcholine sterase gene (ace1) from the mosquito *Aedes aegypti* with implications for comparative genome analysis. Insect Biochem Mol Biol. 2007;37:667-674.

15. Carlier PR, Anderson TD, Wong DM, Hsu DC, Hartsel J, et al. Towards a species-selective acetylcholinesterase inhibitor to control the mosquito vector of malaria, *Anopheles gambiae*. *Chem Biol Interact*. 2008;175:368-375.
16. Jiang H, Liu S, Zhao P, Pope C. Recombinant expression and biochemical characterization of the catalytic domain of acetylcholinesterase-1 from the African malaria mosquito, *Anopheles gambiae*. *Insect Biochem Mol Biol*. 2009;39:646-653.
17. Zhao P, Wang Y, Jiang H. Biochemical properties, expression profiles, and tissue localization of orthologous acetylcholinesterase-2 in the mosquito, *Anopheles gambiae*. *Insect Biochem Mol Biol*. 2013;43:260-271.
18. Engdahl C, Knutsson S, Fredriksson SA, Linusson A, Bucht G, et al. Acetylcholinesterases from the disease vectors *Aedes aegypti* and *Anopheles gambiae*: Functional characterization and comparisons with vertebrate orthologues. *PLoS One*. 2015;10:e0138598.
19. Alout H, Labbe P, Berthomieu A, Djogbénou L, Leonetti JP, et al. Novel AChE inhibitors for sustainable insecticide resistance management. *PloS One*. 2012;7:e47125.
20. Knutsson S, Kindahl T, Engdahl C, Nikjoo D, Forsgren N, et al. N-Aryl-N'-ethyleneaminothioureas effectively inhibit acetylcholinesterase 1 from disease-transmitting mosquitoes. *Eur J Med Chem*. 2017;134:415-427.
21. Knutsson S, Engdahl C, Kumari R, Forsgren N, Lindgren C. Non-covalent inhibitors of mosquito acetylcholinesterase 1 with resistance-breaking potency. *J Med Chem*. 2018;61:10545-10557.
22. Engdahl C, Knutsson S, Ekström F, Linusson A. Discovery of selective inhibitors targeting acetylcholinesterase 1 from disease-transmitting mosquitoes. *J Med Chem*. 2016;59:9409-9421.
23. Mills N. Chem draw ultra 10.0. *J Am Chem Soc*. 2006;128:13649-13650.
24. <http://www.yapcwsoft.com/dd/padeldescriptor/>.
25. Yap CW. PaDEL-descriptor: An open source software to calculate molecular descriptors and fingerprints. *J Comput Chem*. 2011;32:1466-1474.
26. Nandi S, Saxena M, Saxena AK. Identification of therapeutically active molecules against anthrax through structure and ligand based drug design. *Curr Top Med Chem*. 2018;18:1-19.
27. Sharma A, Teotia D, Nandi S. QSAR and structure-based modeling of marine derived anticancer hymenialdisine compounds. *J Develop Drugs*. 2018;7:185-196.
28. Nandi S, Ahmed S, Saxena AK. Combinatorial design and virtual screening of potent anti-tubercular fluoroquinolone and isothiazoloquinolone compounds utilizing QSAR and pharmacophore modeling. *SAR QSAR Environ Res*. 2018;29:151-170.
29. Nandi S, Bagchi MC. QSAR of chalcones utilizing theoretical molecular descriptors. *Curr Comput Aided Drug Des*. 2015;11:184-193.
30. Alam M, Nandi S. QSAR and structure based molecular docking of angelicin compounds: An attempt to drug design against swine influenza. *J Bioanal Biomed*. 2016;8:48-57.
31. Gupta AK, Varshney K, Saxena AK. Toward the identification of a reliable 3D QSAR pharmacophore model for the CCK2 receptor antagonism. *J Chem Inf Model*. 2012;52:1376-1390.
32. Ambure AP, Gajewicz RB, Puzyn AT, Roy K. NanoBRIDGES software, Open access tools to perform QSAR and nano-QSAR modeling. *Chemometr Intell Lab Syst*. 2015;147:1-13.
33. Leardi R. Genetic algorithm in chemometrics and chemistry: A review. *J Chemo*. 2001;15:556-559.
34. Saxena AK, Prathipati P. Comparison of MLR, PLS and GA-MLR in QSAR analysis. *SAR QSAR Environ Res*. 2003;14:433-445.
35. Broadhurst D, Goodacre R, Jones A, Rowland, Kell DB. Genetic algorithms as a method for variable selection in multiple linear regression and partial least squares regression with applications to pyrolysis mass spectrometry. *Anal Chim Acta*. 1997;348:71-86.
36. Hoffman BT, Kopajtic T, Katz JL, Newman AH. 2D QSAR modeling and preliminary database searching for dopamine transporter inhibitors using genetic algorithm variable selection of Molconn Z descriptors. *J Med Chem*. 2000;43:4151-4159.
37. Golbraikh A, Tropsha A. Beware of q². *J Mol Graph Model*. 2002;20:269-276.
38. Gramatica P, Sangion A. A historical excursus on the statistical validation parameters for QSAR models: A clarification concerning metrics and terminology. *J Chem Inf Model*. 2016;pp:1127-1131.
39. Roy K, Mitra I, Kar S, Ojha PK, Das R. Comparative studies on some metrics for external validation of QSPR models. *J Chem Inf Model*. 2012;52:396-408.